ENDOR spectroscopy and DFT calculations: evidence for the hydrogen bond network within α2 in the PCET of *E. coli* ribonucleotide reductase

Supporting Information

Tomislav Argirević[*], Christoph Riplinger[†], JoAnne Stubbe[§], Frank Neese[†] and Marina Bennati[*,¥]

[*] Max Planck Institute for Biophysical Chemistry, 37077 Göttingen, Germany
[†] Max Planck Institute for Chemical Energy Conversion, 45470 Mülheim an der Ruhr, Germany
[§] Dept. of Chemistry and Biology, MIT, Cambridge, MA 02139, USA
[¥] Dept. of Chemistry, University of Göttingen, 37077 Göttingen, Germany

Correspondence: *Marina.Bennati@mpibpc.mpg.de; frank.neese@mpi-mail.mpg.de*

Figure S1. DFT model **1** with two waters with $g_x = 2.0049$, $g_y = 2.0041$ and $g_z = 2.0018$.
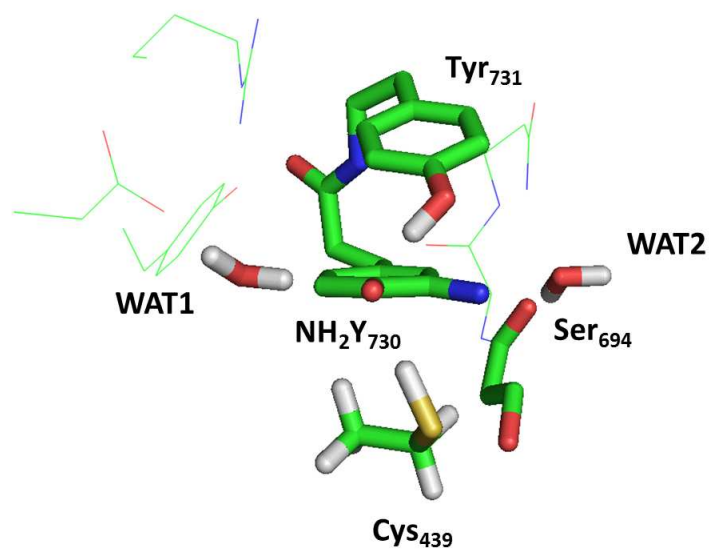

Figure S2. Alternative DFT model **2** with two waters with $g_x = 2.0048$, $g_y = 2.0038$ and $g_z = 2.0018$.
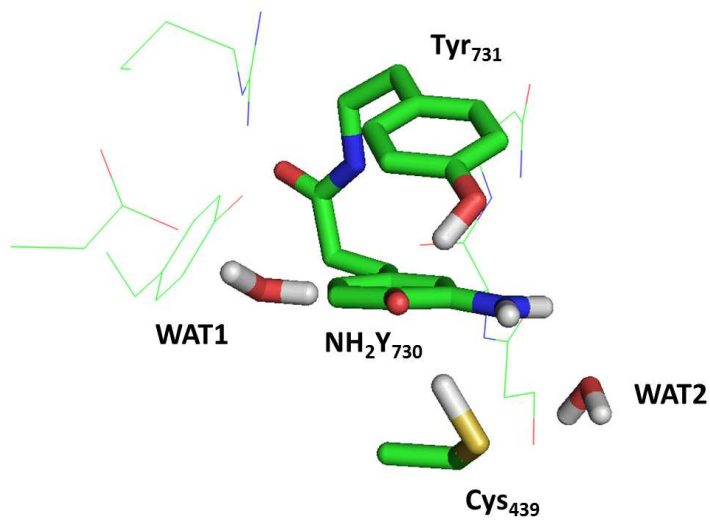
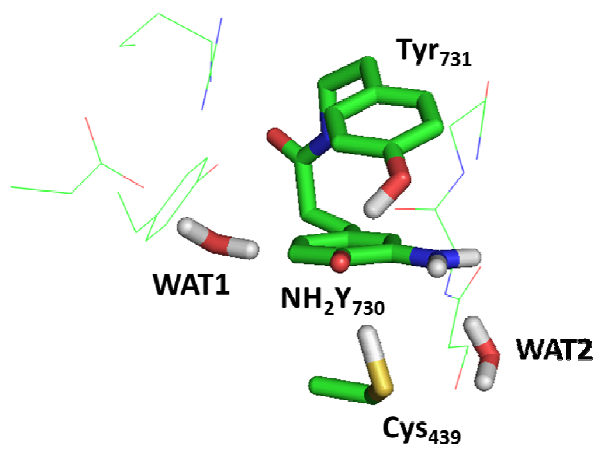**Figure S3.** Alternative DFT model **3** with two waters with $g_x = 2.0055$, $g_y = 2.0041$ and $g_z = 2.0019$.

Fig. S4. Alternative DFT model **5** with one water but shorter HO-**H O**-NH$_2$Y$_{730}$$^\bullet$ distance (1.9 Å) with $g_x = 2.0048$, $g_y = 2.0040$ and $g_z = 2.0018$.
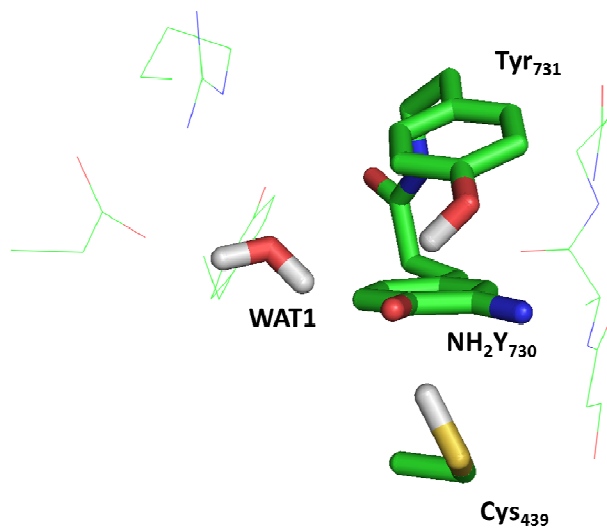
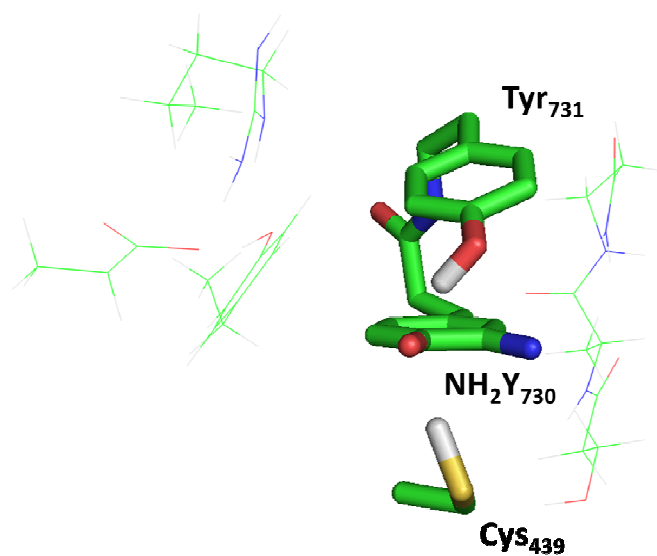**Figure S5.** DFT model **6** without water (see Table 1 for g-values).

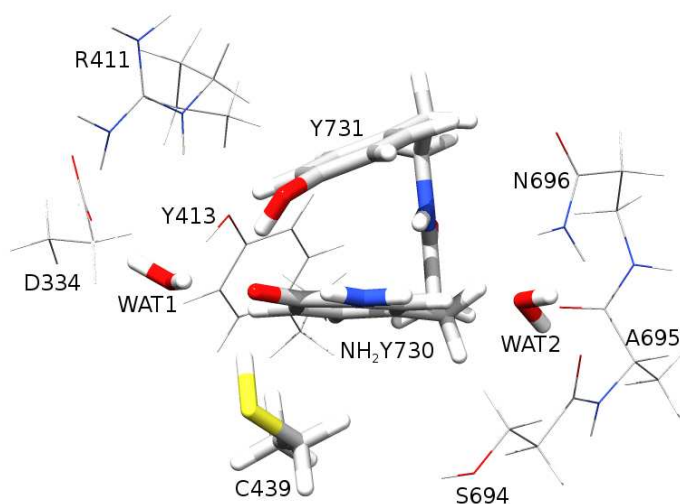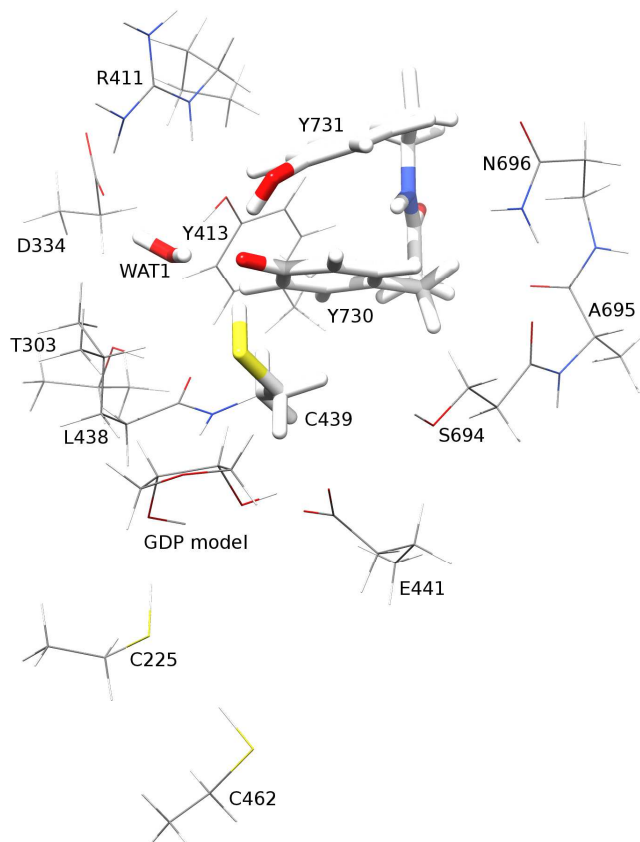**Figure S6.** (a) Cluster model for model **1**. The residues involved in the PCET ($NH_2Y_{730}^{\bullet}$, Y_{731} and C_{439}) and the water molecules are shown in stick representation, the remaining residues are shown in the wire representation.

(b) Cluster model for model **7** with WAT 1 (model **8** is without WAT 1). $Y_{730}^{\bullet}$, Y_{731}, C_{439} and WAT1 are shown in stick representation, the remaining residues are shown in the wire representation. A truncated model for GDP is used in the cluster model structure.

Influence of second sphere residues on hydrogen bond interactions to $NH_2Y_{730}^{\bullet}$

The g-tensor calculations on model systems of different size and composition (see Table 2) show a substantial effect of the second sphere residues on the g_x-value (compare entries 2 and 4). Analyzing the structural properties it can be seen that, when removing these outer residues, the hydrogen bond between the central phenoxy group and WAT1 shrinks significantly by about 0.4 Å (from 2.16 Å in entry 2 to 1.78 Å in entry 4). This suggests that the influence of the surrounding residues on the calculated g-tensor can be rationalized by their steric influence on the hydrogen bonds to the oxygen of $NH_2Y_{730}^{\bullet}$. In order to analyse this further we additionally calculated the g-values as a function of the WAT1-$NH_2Y_{730}^{\bullet}$ hydrogen bond

distance using the small model shown in Table 2, entry 4. The results of this calculation are shown in Figure S7. It can be seen that the g_x-value is a steep function of the hydrogen bond distance. At a short hydrogen bond length of 1.8 Å (as in the small model, entry 4 in Table 2) we have a similar g_x-value as in the small model, at a hydrogen bond distance of 2.2 Å (as in the large model, Table 2, entry 2) the g_x-value of the large model is reached. At an even longer hydrogen bond distance of 3.0 Å the "water-free limit" of the g_x-value is reached – as in the small model without WAT1 (Table 2, entry 5) and in the large model without WAT1 (Table 2, entry 3). Summing up these results it can be concluded that the g_x-value is a sensitive function of the WAT1-NH$_2$Y$_{730}$$^\bullet$ hydrogen bond distance and at the same time the strength of this hydrogen bond is strongly influenced by the interaction of WAT1 with the surrounding second sphere residues, i.e. the effect of the second sphere residues on the g_x-value is of steric nature, modulating the strength of the WAT1-NH$_2$Y$_{730}$$^\bullet$ hydrogen bond, and herewith influencing the g_x-value.

Figure S7. g_x value as a function of the hydrogen bond distance between Y$_{730}$ and WAT1. A relaxed surface scan was carried out with model NH$_2$Y$_{730}$$^\bullet$ – Y$_{731}$ – C$_{439}$–WAT1 (Table 2, entry 4) constraining the distance between O(Y$_{730}$) and H(WAT1).
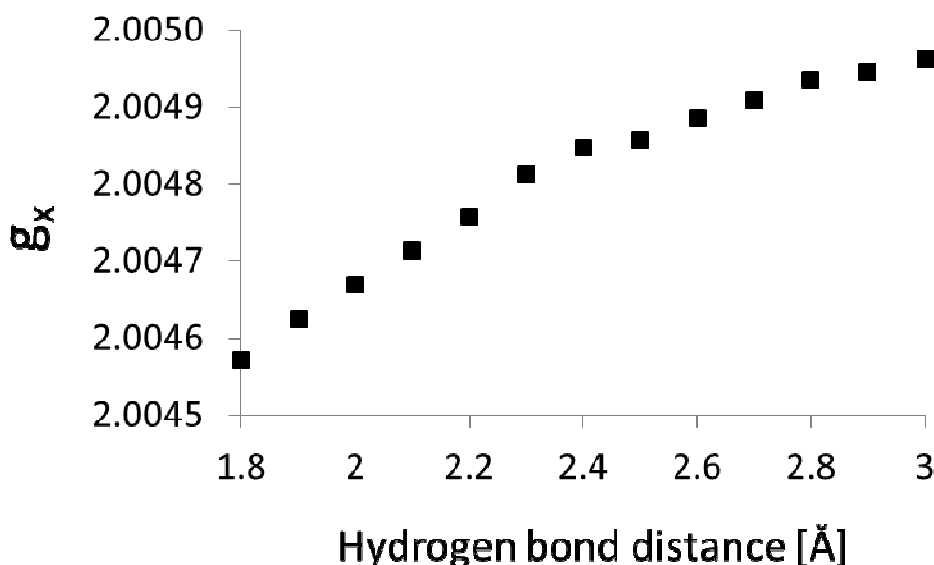
Figure S8. Overlaying structures 2X0X (red, X-ray resolution 2.3 Å), 2XO4 (blue, X-ray resolution 2.5 Å) and 4R1R (green, X-ray resolution 3.2 Å) (10, 32, 33). Only the residues used in model **7** (Figure S6) were used for the overlaying procedure and are displayed. In the overlay procedure the C_α atoms of 2XO4 and 4R1R are fitted onto the respective C_α atoms of 2X0X in such a way, that the RMS deviation of their distances is smallest using the "Pair Fitting" method in PyMOL (Version 1.4.1). The RMS deviation of the pairwise C_α atom distances is a measure for the similarity of the backbone structures. Note that GDP and WAT1 are not used in the overlay procedure and in the calculation of the RMS deviation. The RMS deviation of 2XO4 to 2X0X is 0.106 Å and the RMS deviation of 4R1R to 2X0X is 0.201 Å. All three structures are thus quite similar regarding their backbones. The visualized overlay shows, that also the side chain orientations are similar. Only the side chain of C225 in 4R1R shows small rearrangements compared to 2X0X and 2XO4, which is due to the binding of the substrate.
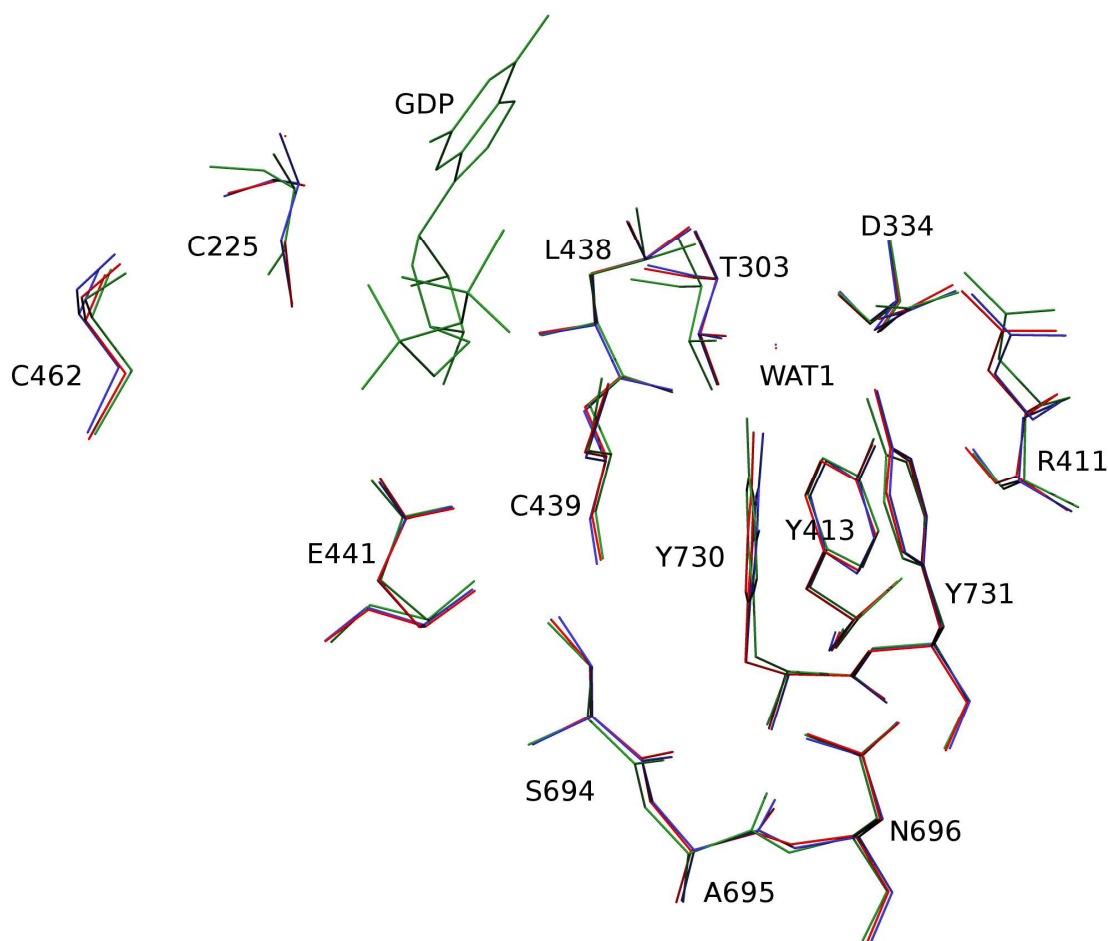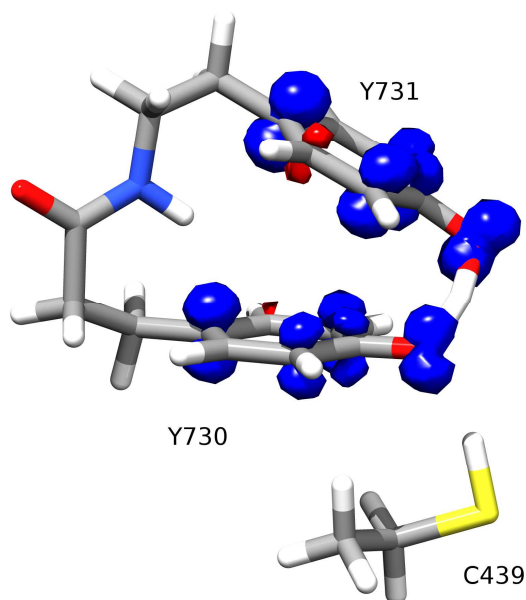
Figure S9. **(a)** Spin density plot (isocontour surfaces for $+0.005/Å^3$ and $-0.005/Å^3$ are shown as blue and red surface representations) for the $Y_{731} \leftrightarrow Y_{730}$ radical transfer transition state structure. Model **7** (Figure S6b) was used for the calculations. For better visualization only the PCET residues are shown.

(b) Spin density plot (isocontour surfaces for $+0.005/Å^3$ and $-0.005/Å^3$ are shown as blue and red surface representations) for the $Y_{730} \leftrightarrow C_{439}$ radical transfer transition state structure. Model **7** (Figure S6b) was used for the calculations. For better visualization only the PCET residues are shown.

S8